Supplementary Information (SI) for Chemical Science.
This journal is © The Royal Society of Chemistry 2026

Supporting Information for

Manipulating excited-state dynamics through macrocycle positioning in a rotaxane for sensitive and discriminative methanol sensing

Yu Wang, Yalei Ma, Ruijuan Wen, Jing Li, Taihong Liu, Liping Ding, Rong Miao,* and Yu Fang

Key Laboratory of Applied Surface and Colloid Chemistry, Ministry of Education, Shaanxi Provincial Key Laboratory of New Concept Sensors and Molecular Materials, School of Chemistry and Chemical Engineering,
Shaanxi Normal University, Xi'an 710119, P. R. China
Corresponding author: miaorong2015@snnu.edu.cn

1. Materials and instrumentation

All chemicals were used without further purification unless otherwise specified. 4-Bromo-1, 8-naphthalic anhydride (Leyan), 7-Aminoheptanoic acid (Leyan), 1-Methyl-1H-indol-2-yl-2-boronic acid (Leyan), Potassium carbonate (SCR), Bis(triphenylphosphine)palladium(II) dichloride ($PdCl_2(PPh_3)_2$) (Bidepharm), 4-Nitrophenol (Macklin), 1-(3-Dimethylaminopropyl)-3-ethylcarbodiimide (Leyan), 3, 5-Bis(trifluoromethyl)benzylamine (Macklin), 1-(3-Dimethylaminopropyl)-3-ethylcarbodiimide hydrochloride (Leyan), Dibenzo-24-crown-8 (Macklin), 2, 2-dimethyl-propanoylchlorid (Macklin) were obtained from commercial suppliers. Analytical grade solvents, including acetonitrile (ACN), triethylamine (Et_3N), hexane (Hex), toluene (Tol), 1, 4-dioxane (Diox), tetrahydrofuran (THF), ethyl acetate (EtOAc), trichloromethane (TCM), dichloromethane (DCM), acetone (ACE), dimethylformamide (DMF), dimethylsulfoxide (DMSO), ethanol (EtOH), methanol (MeOH), were purchased from China Sinopharm Chemical Reagent Co., Ltd.

Proton nuclear magnetic resonance spectra (^{1}H NMR), fluorine nuclear magnetic resonance (^{19}F NMR) and carbon nuclear magnetic resonance spectra (^{13}C NMR) spectra were obtained on a Bruker AV 600 NMR spectrometer. High-resolution mass spectra (HRMS) were obtained from Bruker high-resolution LC-MS with electrospray ionization (ESI). UV-vis absorption measurements were measured on a U-3900 (Hitachi) spectrophotometer. Fluorescence measurements were carried out on an FLS 980 spectrometer (Edinburgh). Fluorescence quantum yields were obtained on a quantum efficiency measurement system (Hamamatsu, Quantaurus-QY). Single crystal X-ray diffraction (XRD) was collected on Bruker APEX-II CCD diffractometer.

2. Synthesis

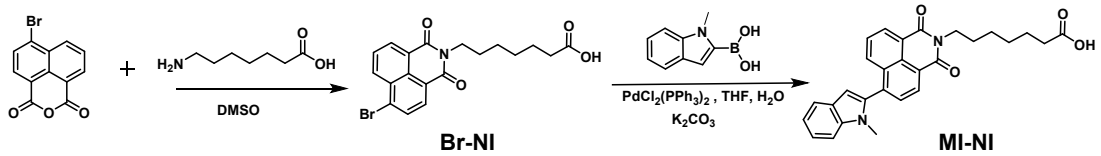

2.1 Synthesis of MI-NI

Scheme S1. Synthesis route of MI-NI.

1.38 g of 4-bromo-1, 8-naphthalic anhydride (5 mmol) was dissolved in 40 mL DMSO. 0.75 g of 7-aminoheptanoic acid was added to the solution and the mixture was heated to reflux. After 2 h, the mixture was cooled down. The precipitate was filtrated and repeatedly washed with water and ethanol. 1.92 g (yield: 95%) of Br-NI was obtained as while solids.

MI-NI was synthesized through the Suzuki coupling reaction. A 50 mL two-neck flask was charged with Br-NI (0.36 g, 0.8 mmol), potassium carbonate (148 mg, 1.2 mmol), and 1-Methyl-1H-indol-2-yl-2-boronic acid (168 mg, 0.96 mmol). $PdCl_2(PPh_3)_2$ (56 mg, 0.08 mmol) were added to the mixture under nitrogen. Afterwards, THF (10 mL) and H_2O (10 mL) were added to the mixture, and the reaction mixture was allowed to stir at 65 °C for 12 h under nitrogen. Afterwards, DCM (10 mL) and H_2O (10 mL) were added to the mixture. The aqueous layer was extracted with DCM (3 × 20 mL). The organic layer was collected and dried with anhydrous Na_2SO_4. The crude product was purified by column chromatography using dichloromethane/methanol (80:1) on a silica gel column. MI-NI was obtained as yellow solids (290 mg, yield: 82%).

2.2 Synthesis of MI-NI-N

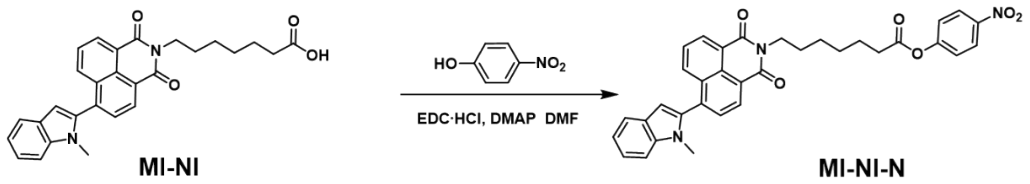

Scheme S2. Synthesis route for MI-NI-N.

In a l00 mL round bottomed flask, MI-NI (0.27 g, 0.6 mmol), 4-nitrophenol (0.13 g, 0.9 mmol) and 1-(3-Dimethylaminopropyl)-3-ethylcarbodiimide (35 mg, 0.29 mmol), were dissolved in anhydrous DMF (10 mL). Then, EDC·HCl (0.17 g, 0.9 mmol) was carefully added and the mixture was stirred for 12 h at room temperature. When the reaction was completed, H_2O (100 mL) and ethyl acetate (20 mL) were added. The aqueous layer was extracted with ethyl acetate (3 × 40 mL). The combined organic layers were washed with LiCl (15% *w*/*v*, 3 × 100 mL) and brine (40 mL). The organic layer was collected and dried with anhydrous Na_2SO_4. Purification of the crude product was achieved by column chromatography using dichloromethane/hexane (20:1) on a silica gel column. NI-MI-N was obtained as yellow solid (260 mg, yield: 75%).

2.3 Synthesis of Axle

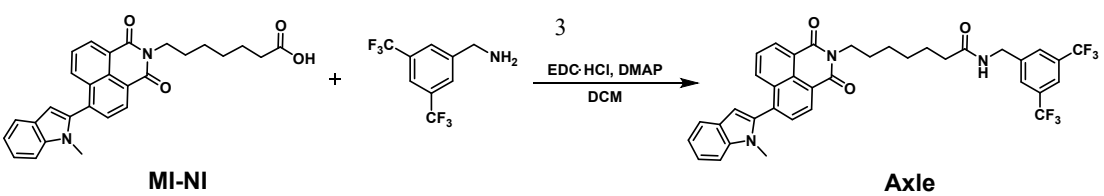

Scheme S3. Synthesis route for the free axle.

In a 5 mL round bottomed flask, MI-NI (227 mg, 0.5 mmol), 3, 5-bis(trifluoromethyl)benzylamine (121 mg, 0.9 mmol) and DMAP (61 mg, 0.5 mmol) were dissolved in anhydrous DCM (5 mL). EDC·HCl (105 mg, 0.55 mmol) was carefully added to the reaction and the mixture was stirred for 4 h at room temperature. When the reaction was completed, the solvent was removed under reduced pressure. Purification of the crude product was achieved by column chromatography using ethyl acetate/hexane (1:3) on a silica gel column. Axle was obtained as yellow solid (290 mg, yield: 85%). ^{1}H NMR (600 MHz, CD_2Cl_2) δ = 8.61 (dd, *J*=21.1, 7.3, 2H), 8.21 (d, *J*=8.5, 1H), 7.89 - 7.63 (m, 6H), 7.46 (d, *J*=8.1, 1H), 7.33 (t, *J*=7.7, 1H), 7.20 (t, *J*=7.5, 1H), 6.73 (s, 1H), 6.17 (s, 1H), 4.55 (d, *J*=6.1, 2H), 4.22 - 4.13 (m, 2H), 3.56 (s, 3H), 2.28 (t, *J*=7.5, 2H), 1.84 - 1.66 (m, 4H), 1.51 (d, *J*=39.3, 4H). ^{13}C NMR (600 MHz, $CDCl_3$) δ (ppm) 173.31, 164.22, 164.02, 141.45, 138.38, 137.16, 136.98, 132.78, 132.06, 131.83, 131.44, 131.30, 130.37, 129.50, 128.53, 127.90, 127.79, 127.44, 124.14, 122.92, 122.68, 122.63, 122.33, 121.37, 120.95, 120.45, 109.77, 105.15, 77.24, 77.03, 76.82, 42.68, 40.15, 36.42, 31.19, 29.71, 28.52, 27.64, 26.49, 25.36. HRMS calculated for $[C_{37}H_{32}F_6N_3O_3]^+$: 680.2342; Found: 680.2347.

2.4 Synthesis of R-2

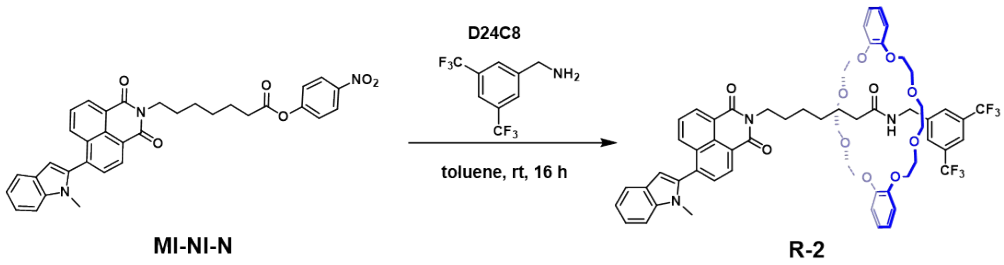

Scheme S4. Synthesis route for R-2.

MI-NI-N (80.5 mg, 0.14 mmol), 3, 5-bis(trifluoromethyl)benzylamine (34 mg, 0.14 mmol) and D24C8 (62.8 mg, 14 mmol) were dissolved in toluene (1 mL) and the mixture was stirred at room temperature. After 16 h, the solvent was removed under reduced pressure. The crude product was purified by column chromatography using dichloromethane/methanol (125:1) on a silica gel column. R-2 was obtained as bright green solid (94 mg, yield: 60%). ^{1}H NMR (600 MHz, CD_2Cl_2) δ (ppm) 8.67 - 8.58 (m, 2H), 8.40 (s, 2H), 8.21 (t, *J*=9.6, 1H), 7.81 (d, *J*=7.4, 1H), 7.56 (s, 1H), 7.46 (d, *J*=8.2, 1H), 7.32 (t, *J*=7.7, 1H), 7.25 (s, 1H), 7.20 (t, *J*=7.5, 1H), 6.80 - 6.60 (m, 9H), 4.85 (d,

J=3.6, 2H), 4.21 - 4.14 (m, 2H), 4.06 - 3.95 (m, 8H), 3.85 - 3.75 (m, 4H), 3.68 - 3.57 (m, 8H), 3.56 (s, 3H), 3.31 (dd, *J*=10.4, 6.3, 4H), 2.15 - 2.07 (m, 2H), 1.70 (dt, *J*=15.3, 7.6, 2H), 1.61 -1.51 (m, 2H), 1.41 - 1.33 (m, 2H), 1.30 (dd, *J*=14.6, 7.5, 2H). ^{13}C NMR (600 MHz, $CDCl_3$) δ (ppm) 172.16, 164.09, 163.89, 147.46, 141.88, 138.36, 137.02, 132.64, 131.69, 131.36, 131.30, 130.29, 129.49, 128.92, 128.71, 128.52, 127.90, 127.42, 124.78, 123.04, 122.97, 122.76, 122.65, 120.93, 120.43, 120.34, 118.91, 111.29, 111.20, 109.75, 105.08, 77.25, 77.04, 76.82, 70.79, 70.67, 69.82, 69.68, 67.81, 67.69, 43.49, 40.50, 36.25, 31.59, 31.19, 29.55, 28.15, 27.06, 25.81, 22.66, 14.11. HRMS calculated for $[C_{61}H_{64}F_6N_3O_{11}]^+$: 1128.4440; Found: 1128.4438.

2.5 Synthesis of the R-1 and R-3

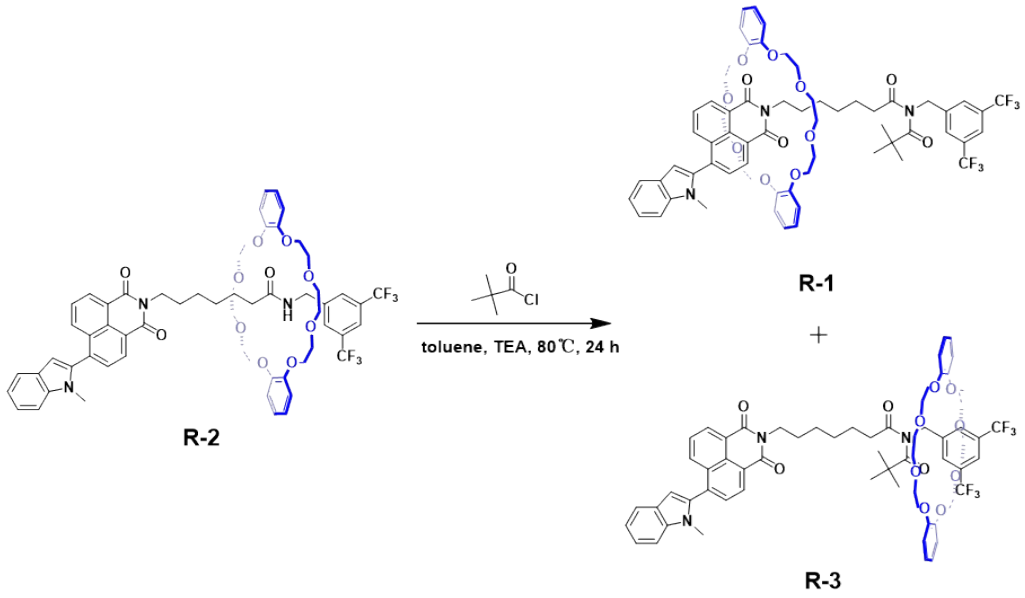

Scheme S5. Synthesis route for R-1 and R-3.

To a stirred solution of R-2 (56.6 mg, 0.05 mmol), triethylamine (20 μL, 0.02 mmol) in 2 mL of toluene at room temperature, pivaloyl chloride (120 μL, 0.1 mmol) was added dropwise. Then the reaction mixture was maintained at 80 °C for 24 h. Upon completion, the reaction mixture was washed with 5% HCl (aqueous solution), 5% $NaHCO_3$ (aqueous solution) and water. The organic layer was collected and dried with anhydrous Na_2SO_4. Then the solvent was removed by rotary evaporation. The crude product was purified by column chromatography using ethyl acetate/hexane (1:2) on a silica gel column.

R-1: Light green solid (14 mg, yield: 23%). ^{1}H NMR (600 MHz, CD_2Cl_2) δ (ppm) 8.54 (dd, *J* = 18.3, 7.3 Hz, 3H), 8.13 (d, *J* = 8.5 Hz, 1H), 7.75 (d, *J* = 7.5 Hz, 1H), 7.67 (dt, *J* = 17.3, 8.4 Hz, 4H), 7.45 (d, *J* = 8.2 Hz, 1H), 7.41 (s, 2H), 7.32 (t, *J* = 7.7 Hz, 1H),

7.19 (t, *J* = 7.5 Hz, 1H), 6.76 - 6.62 (m, 9H), 4.53 (s, 2H), 4.08 (dd, *J* = 10.3, 4.9 Hz, 4H), 4.03 - 3.97 (m, 4H), 3.96 - 3.90 (m, 2H), 3.86 - 3.75 (m, 8H), 3.69 - 3.62 (m, 4H), 3.62 - 3.56 (m, 4H), 3.53 (s, 3H), 3.06 - 2.98 (m, 2H), 2.09 (s, 2H), 1.62 (dt, *J* = 15.2, 7.7 Hz, 2H), 1.55 (d, *J* = 9.6 Hz, 2H), 1.52 - 1.45 (m, 3H), 1.08 (d, *J* = 25.7 Hz, 9H). ^{13}C NMR (600 MHz, $CDCl_3$) δ (ppm) 188.44, 179.02, 163.88, 163.68, 148.18, 141.61, 138.29, 137.13, 136.56, 132.21, 131.15, 130.99, 129.92, 129.30, 127.88, 127.31, 127.22, 123.03, 122.58, 120.90, 120.48, 120.39, 120.28, 111.76, 109.72, 104.96, 77.23, 77.02, 76.81, 71.29, 71.00, 69.90, 68.22, 47.89, 43.36, 40.96, 36.18, 31.14, 29.70, 29.01, 28.83, 28.76, 28.52, 27.82, 26.52, 23.95, 22.65, 14.11. HRMS calculated for $[C_{66}H_{71}F_6N_3O_{12}Na]^+$: 1234.4834; Found: 1234.4839.

R-3: Light yellow solid (18 mg, yield: 30%). ^{1}H NMR (600 MHz, CD_2Cl_2) δ (ppm) 8.67 - 8.61 (m, 3H), 8.60 (d, *J* = 7.2 Hz, 1H), 8.21 (d, *J* = 8.5 Hz, 1H), 7.82 (d, *J* = 7.4 Hz, 1H), 7.76 - 7.68 (m, 2H), 7.51 (s, 1H), 7.46 (d, *J* = 8.3 Hz, 1H), 7.33 (s, 1H), 7.20 (t, *J* = 7.5 Hz, 1H), 6.85 - 6.71 (m, 9H), 4.87 (ddd, *J* = 18.6, 15.3, 3.8 Hz, 3H), 4.15 - 4.00 (m, 8H), 3.91 (dd, *J* = 10.8, 6.1 Hz, 2H), 3.78 - 3.67 (m, 4H), 3.62 (dd, *J* = 11.2, 6.4 Hz, 3H), 3.56 (s, 3H), 3.54 - 3.35 (m, 8H), 3.24 - 3.14 (m, 2H), 3.10 (dd, *J* = 9.2, 5.8 Hz, 2H), 1.86 (ddd, *J* = 53.1, 26.5, 22.4 Hz, 2H), 1.74 (s, 4H), 1.57 (dt, *J* = 15.1, 7.4 Hz, 2H), 1.26 (s, 2H), 0.94 (s, 9H). ^{13}C NMR (600 MHz, $CDCl_3$) δ (ppm) 169.19, 163.99, 163.79, 148.11, 148.04, 141.99, 138.35, 136.99, 136.06, 135.46, 132.63, 131.29, 130.23, 129.47, 129.27, 129.06, 128.48, 127.89, 127.41, 122.66, 120.93, 120.80, 120.67, 120.43, 112.21, 111.79, 109.74, 105.09, 77.22, 77.01, 76.80, 70.66, 70.51, 69.73, 69.59, 68.25, 67.98, 53.62, 44.48, 44.05, 40.45, 31.58, 31.17, 30.08, 28.26, 27.99, 27.56, 26.04, 22.64, 14.10. HRMS calculated for $[C_{66}H_{72}F_6N_3O_{12}]^+$: 1212.5015; Found: 1212.5022.

3. Sensing film fabrication and sensing performance study

3.1 Fabrication of sensing films. Sensing film was prepared by drop-casting of 60 μL corresponding compounds (free axle or R-2) solution (1 mg/mL in $CHCl_3$) onto a piece of quartz glass (*d* = 12.5 mm). The films were left to dry at ambient condition for 24 h before sensing performance tests.

3.2 Details for sensing performance study. The sensing tests were carried out on a home-made sensing platform (Figure 6a) with an excitation source of 402 nm LED light. With the platform, fluorescence intensity of the films could be monitored

continuously. Analyte vapors with different methanol concentration were prepared by mixing certain amounts of saturated methanol vapors with air. The vapor concentrations were calculated according to their saturated pressures. The pulsed sampling process was aided by a mini pump with a sampling volume of 25 mL. For repeated tests, fresh air was used as the carrier gas to remove the analytes from the film.

3.3 Limit of detection calculation. The limit of detection was determined using the signal-to-noise approach, $LOD \approx \frac{3N}{S}$, where N is noise standard deviation and S is the slope of the calibration curve. In the experiment, N was calculated based the responses of the film to clean air, and S is the slope of the calibration curve shown in inset of Figure 6c.

4. Supplement figures.

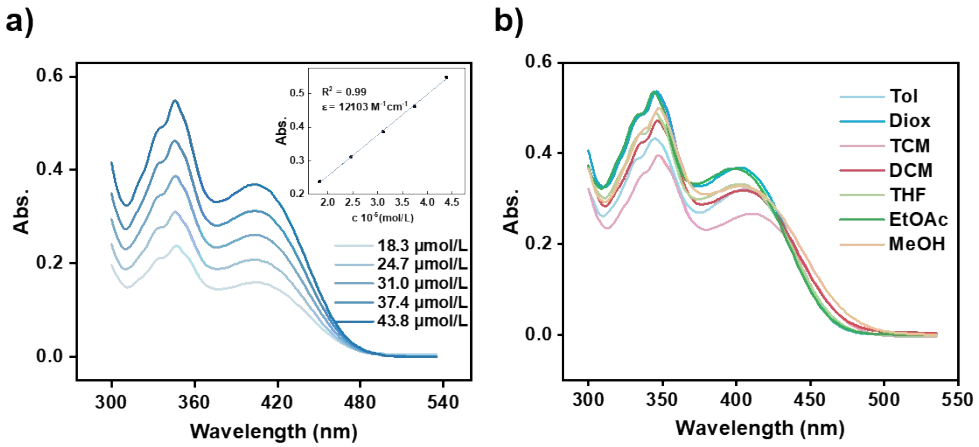

Fig. S1. UV-vis absorption spectra of the free axle in (a) DCM under different concentrations (1.83×10^{-5} M ~ 4.38×10^{-5} M) and in (b) different solvents (2.19×10^{-5} M). Tol: Toluene; Diox: 1, 4-Dioxane; TCM: Trichloromethane; DCM: Dichloromethane; THF: Tetrahydrofuran; EtOAc: Ethyl acetate; MeOH: Methanol.

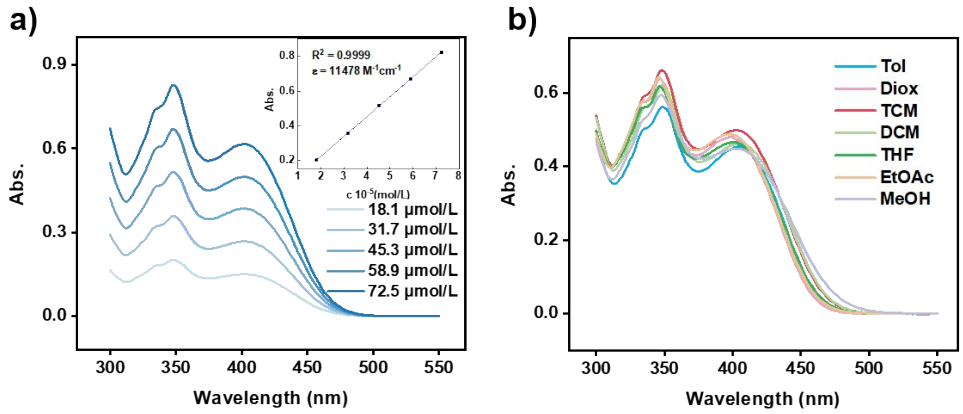

Fig. S2. UV-vis absorption spectra of R-1 in (a) DCM under different concentrations (1.81×10^{-5} M ~ 7.25×10^{-5} M) and in (b) different solvents (5.89×10^{-5} M). Tol: Toluene; Diox: 1, 4-Dioxane; TCM: Trichloromethane; DCM: Dichloromethane; THF: Tetrahydrofuran; EtOAc: Ethyl acetate; MeOH: Methanol.

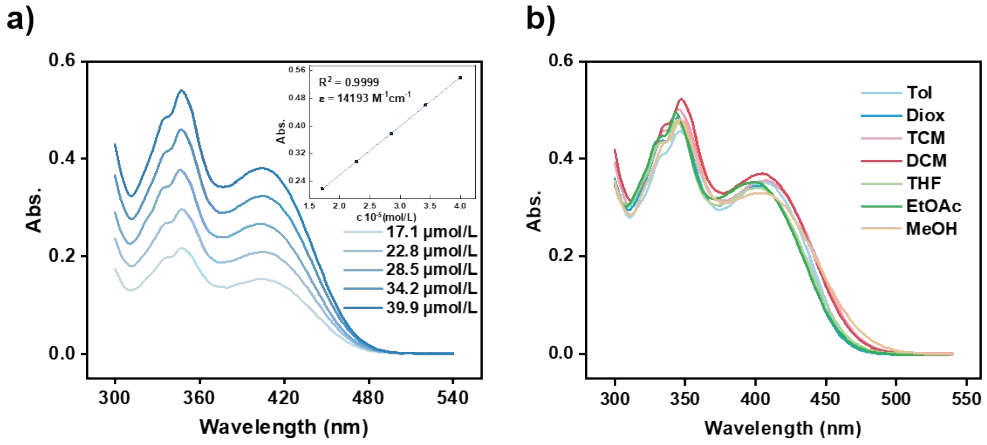

Fig. S3. UV-vis absorption spectra of R-2 in (a) DCM under different concentrations (1.71×10^{-5} M ~ 3.99×10^{-5} M) and in (b) different solvents (3.99×10^{-5} M). Tol: Toluene; Diox: 1, 4-Dioxane; TCM: Trichloromethane; DCM: Dichloromethane; THF: Tetrahydrofuran; EtOAc: Ethyl acetate; MeOH: Methanol.

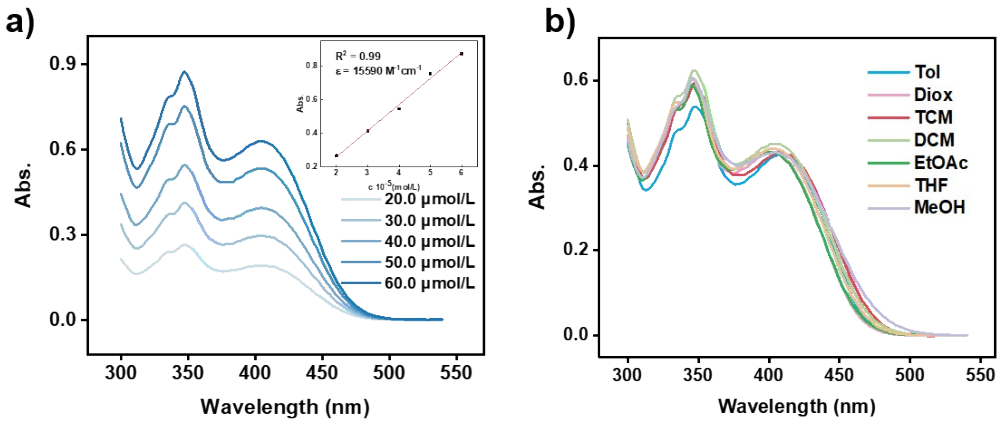

Fig. S4. UV-vis absorption spectra of R-3 in (a) DCM under different concentrations (2.00×10^{-5} M ~ 6.00×10^{-5} M) and in (b) different solvents (5.00×10^{-5} M). Tol: Toluene; Diox: 1, 4-Dioxane; TCM: Trichloromethane; DCM: Dichloromethane; THF: Tetrahydrofuran; EtOAc: Ethyl acetate; MeOH: Methanol.

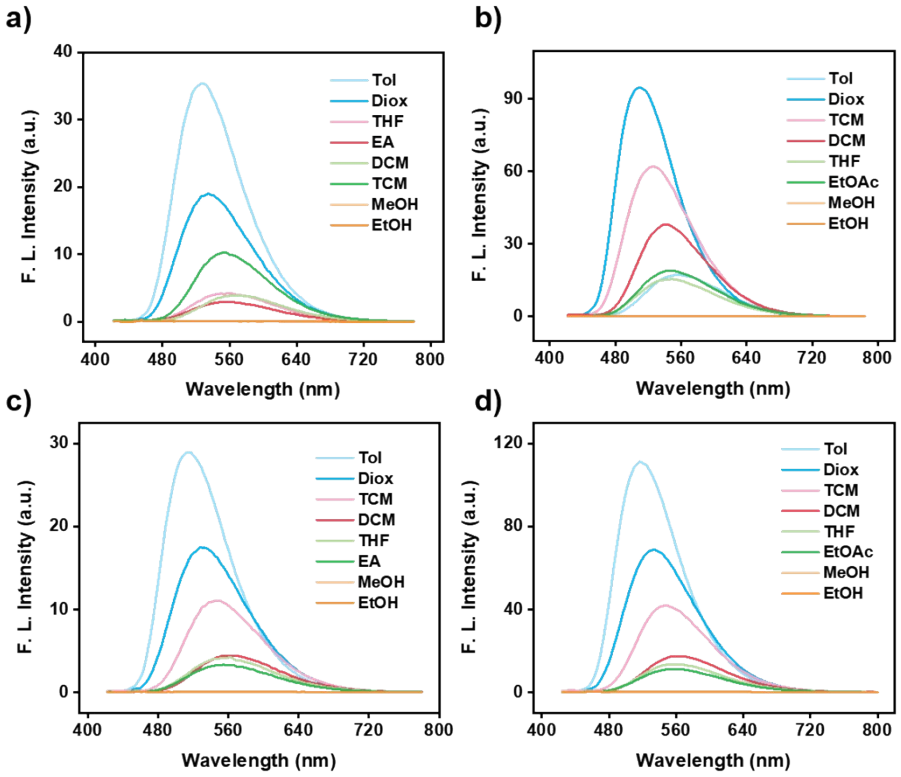

Fig. S5. Fluorescence spectra of the compounds in different solvents: (a) the free axle (λ_{ex} = 402 nm); (b) R-1 (λ_{ex} = 402 nm); (c) R-2 (λ_{ex} = 402 nm); (d) R-3 (λ_{ex} = 404 nm). Tol: Toluene; Diox: 1, 4-Dioxane; TCM: Trichloromethane; DCM: Dichloromethane; THF: Tetrahydrofuran; EtOAc: Ethyl acetate; MeOH: Methanol; EtOH: Ethanol. Compound concentration: 5.00×10^{-6} M.

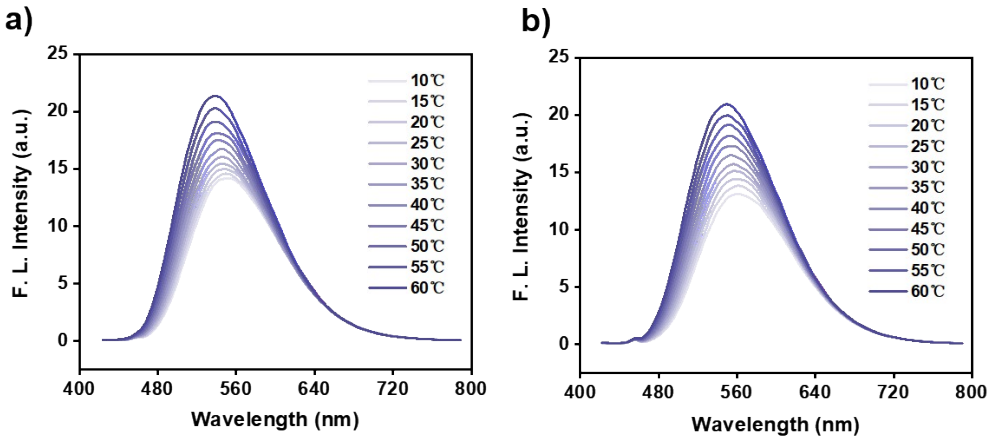

Fig. S6. Fluorescence spectra of the (a) free axle and (b) R-2 in THF under different temperatures (10 ℃ ~ 60 ℃). Compound concentration: 5.00 × 10^{-6} M; λ_{ex} = 402 nm.

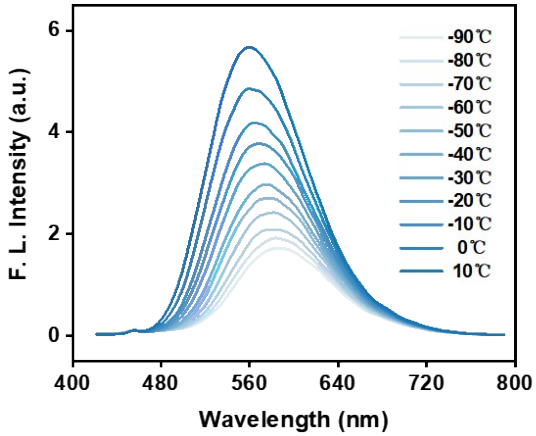

Fig. S7. Fluorescence spectra of R-2 in THF under different temperatures (-90 ℃ ~ 10 ℃. Compound concentration: 5.00 × 10^{-6} M; λ_{ex} = 402 nm.

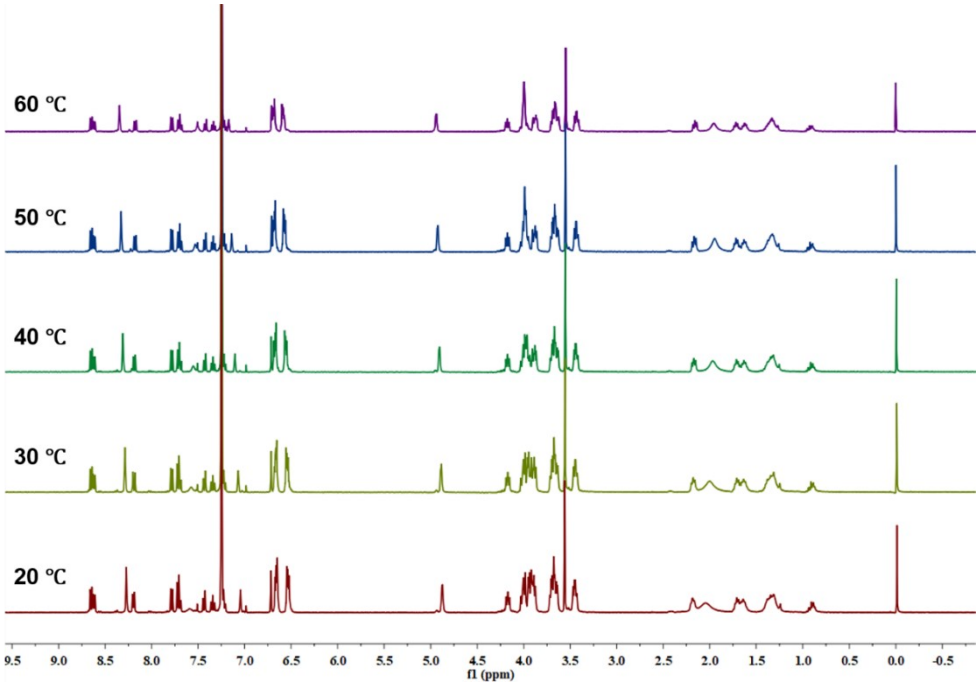

Fig. S8. ^{1}H NMR spectra of R-2 in $CDCl_3$ under different temperatures.

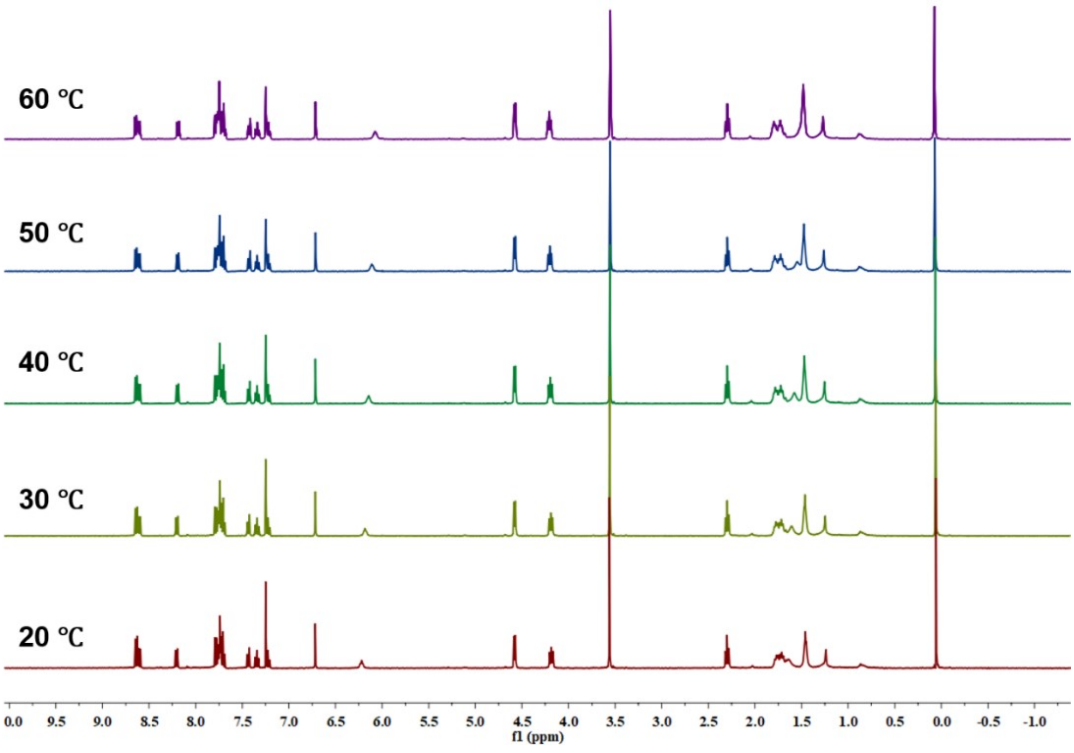

Fig. S9. ^{1}H NMR spectra of the free axle in $CDCl_3$ under different temperatures.

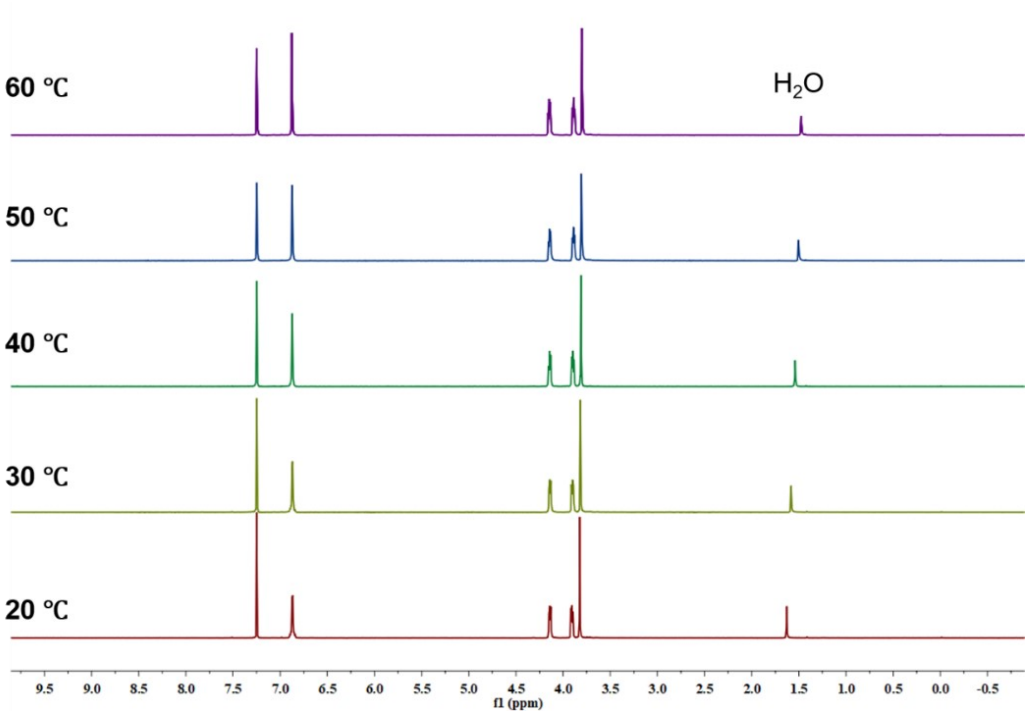

Fig. S10. ^{1}H NMR spectra of D24C8 in $CDCl_3$ under different temperatures.

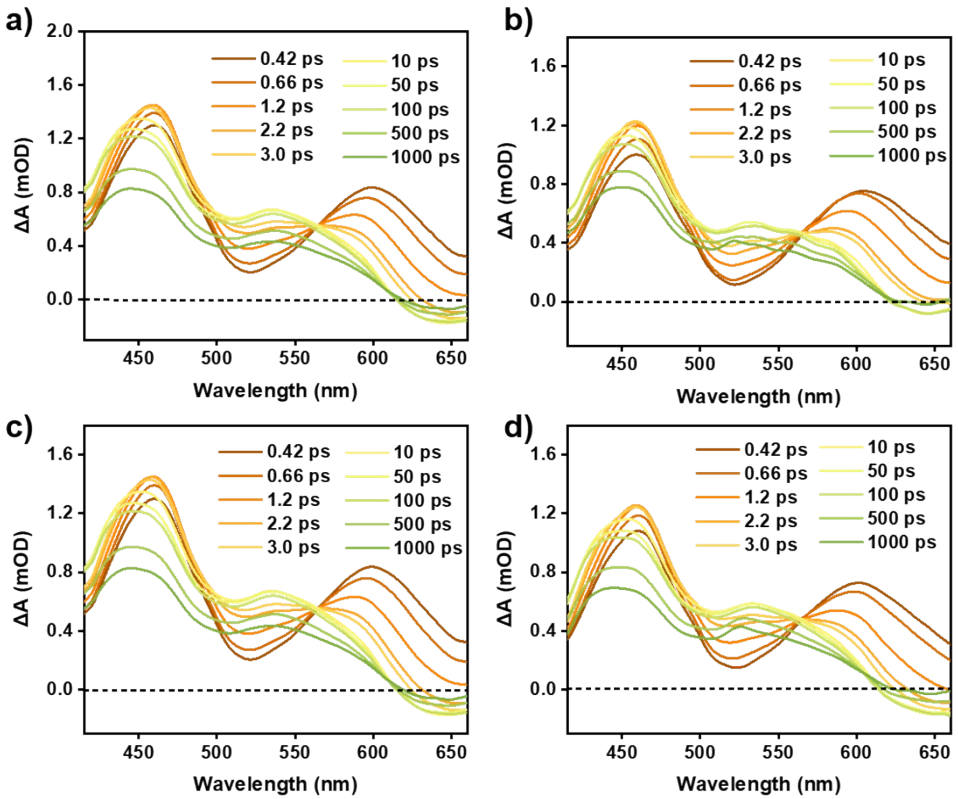

Fig. S11. Fs-TA spectra of the compounds in THF as a function of time delay: (a) the free axle; (b) R-1; (c) R-2; (d) R-3.

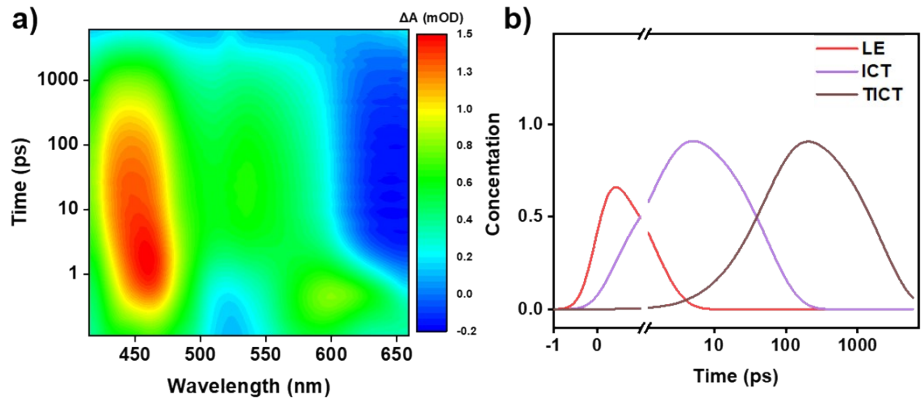

Fig. S12. (a) The fs-TA pseudo-color maps and (b) the distribution of excited-state species as a function of time of R-2 in THF. Compound concentration: 5.00×10^{-5} M. LE: local excited state; ICT: intramolecular charge transfer; TICT: twisted intramolecular charge transfer.

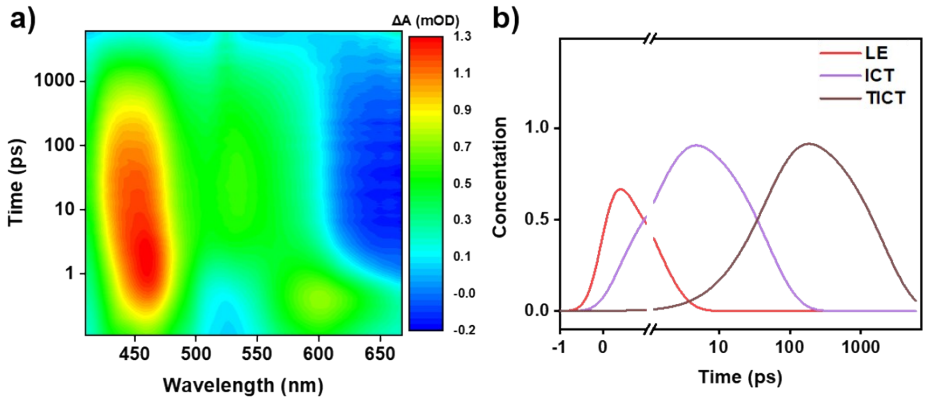

Fig. S13. (a) The fs-TA pseudo-color maps and (b) the distribution of excited-state species as a function of time of R-3 in THF. Compound concentration: 5.00×10^{-5} M. LE: local excited state; ICT: intramolecular charge transfer; TICT: twisted intramolecular charge transfer.

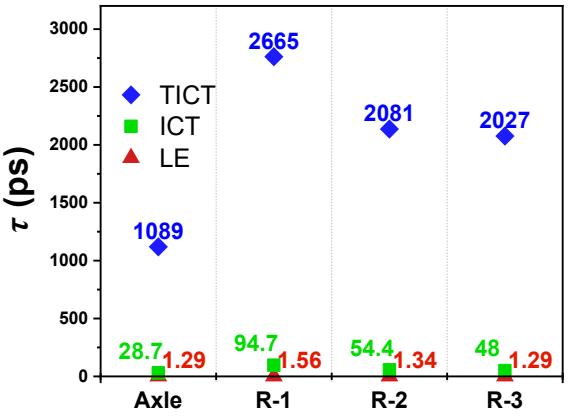

Fig. S14. Lifetime of the excited species (LE, ICT, and TICT) in the four compounds (Axle, R-1, R-2, and R-3).

Table S1. Crystallographic data of R-2 crystals.

Compound	R-2
Empirical formula	$C_{61}H_{64}F_6N_3O_{11}$
Formula weight	1128.14
Temperature/K	223.00
Crystal system	monoclinic
Space group	Cc
a/Å	53.1545(16)
b/Å	12.9581(4)
c/Å	16.6244(4)
α/°	90
β/°	101.771(3)
γ/°	90
Volume/Å^3	11209.8(6)
Z	8
ρ_{calc}g/cm^3	1.337
μ/mm^{-1}	0.883
F(000)	4736.0
Crystal size/mm^3	0.13 × 0.11 × 0.08
Radiation	CuKα (λ=1.54178)
2θrange for data collection/°	6.794 to 124.998
Index ranges	-61≤h≤61, -14≤k≤14, -17≤l≤19
Reflections collected	73316
Independent reflections	17612 [R_{int} = 0.0804, R_{sigma} = 0.0553]
Data/restraints/parameters	17612/1808/1581
Goodness-of-fit on F^2	1.052
Final R indexes [I> = 2σ (I)]	R_1 = 0.0748, wR_2 = 0.2099
Final R indexes [all data]	R_1 = 0.1272, wR_2 = 0.2641
Largest diff. peak/hole / e Å^{-3}	0.58/-0.42
Flack parameter	0.16(16)

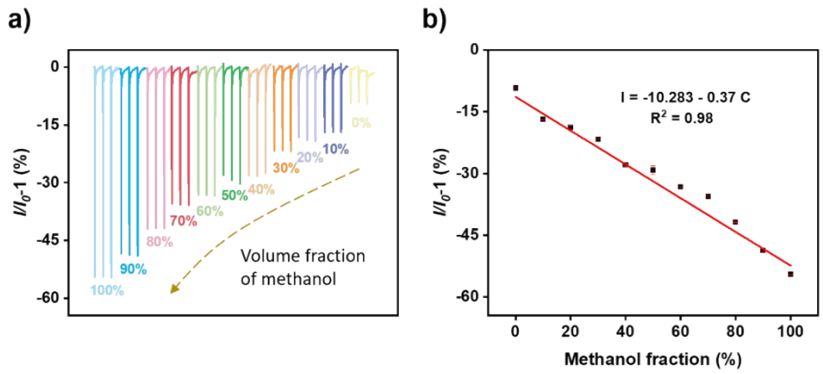

Fig. S15. (a) Response of Film-R to the mixture vapors of methanol and ethanol with different ratios. (b) Linear relationship between the response intensity and the volume fraction of methanol in the mixture. Error bars represent standard deviations from three parallel tests.

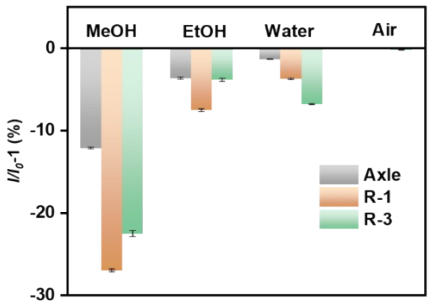

Fig. S16. Fluorescence responses of the film of R-1, R-3 and the axle to methanol, ethanol, water and air. MeOH: Methanol; EtOH: Ethanol.

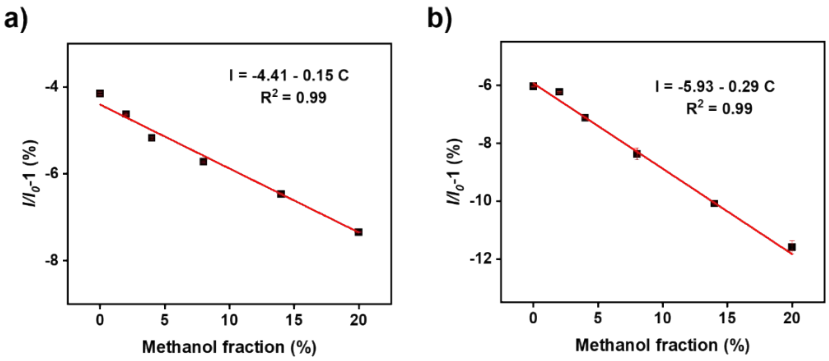

Fig. S17. Linear relationship between response intensity and the volume fraction of methanol in (a) beer (alcohol content 4°) and (b) liquor (alcohol content 52°) with different amounts of methanol. Error bars represent standard deviations from three parallel tests.

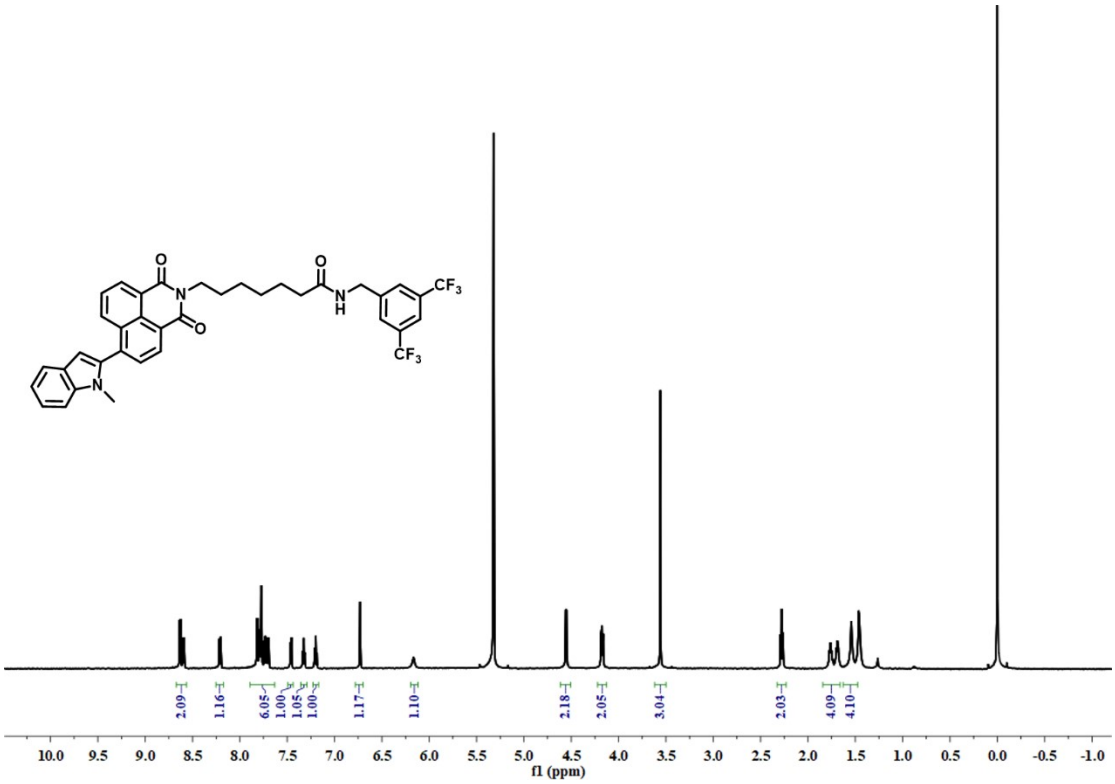

Fig. S18. ^{1}H NMR spectrum of the free axle in CD_2Cl_2.

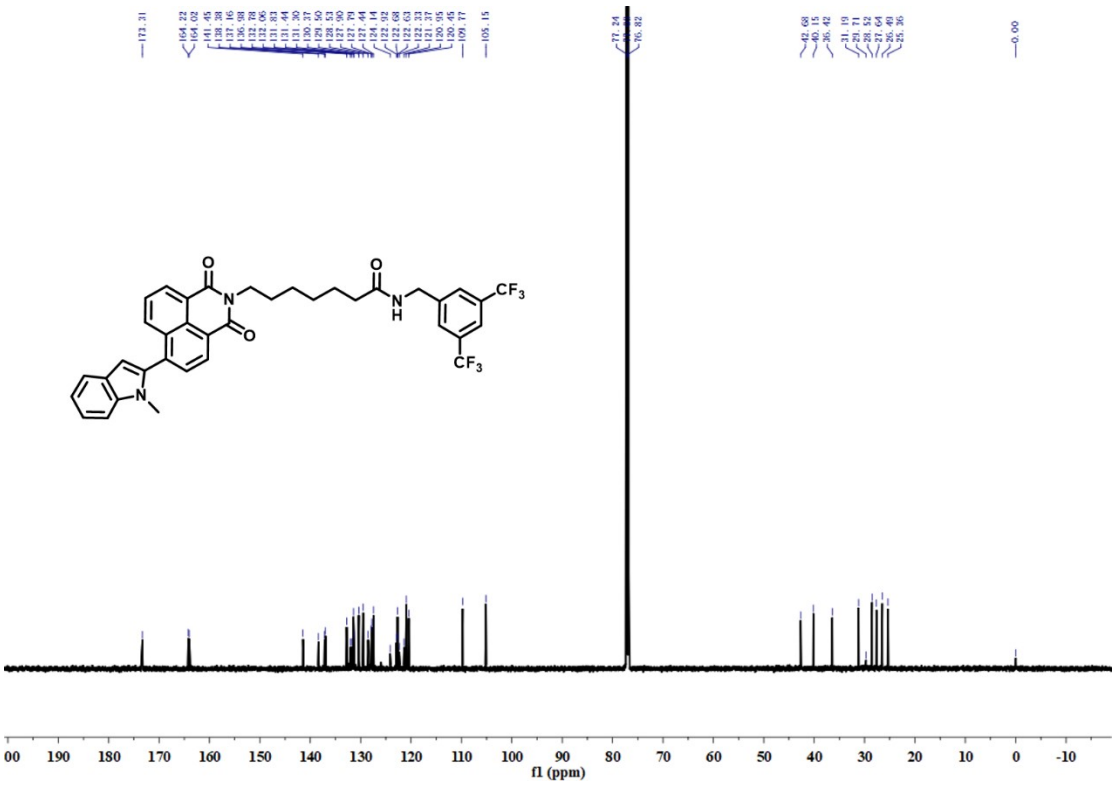

Fig. S19. ^{13}C NMR spectrum of the free axle in $CDCl_3$.

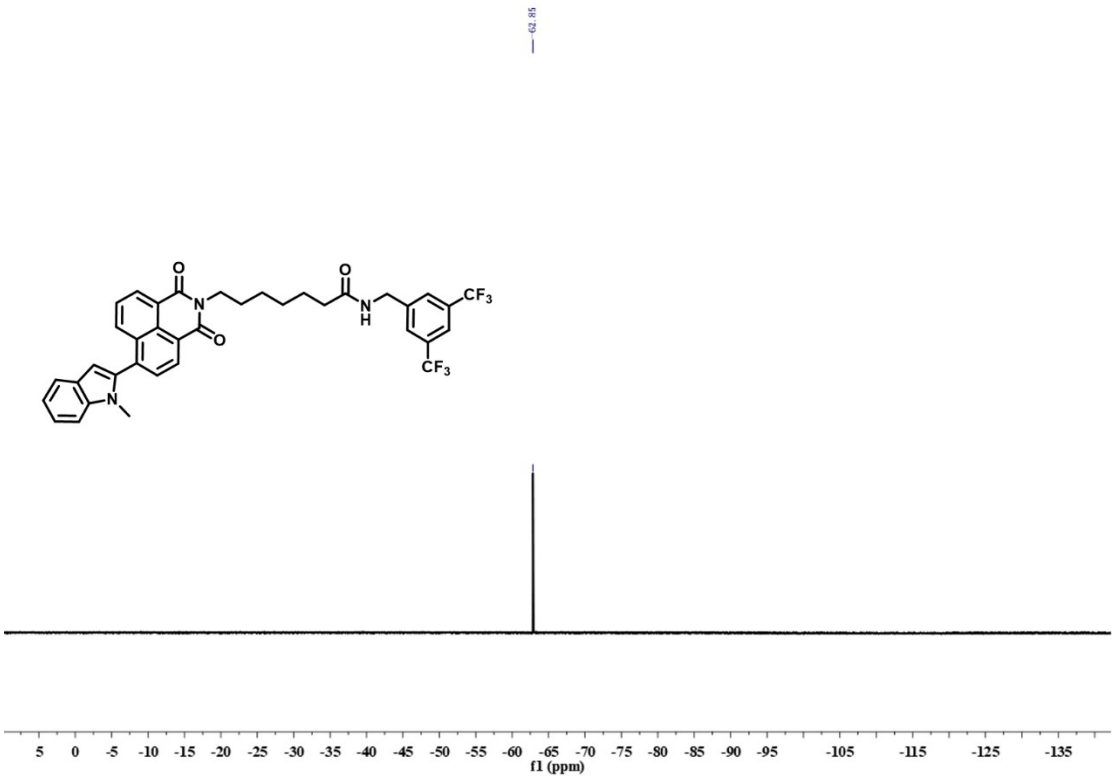

Fig. S20. ^{19}F NMR spectrum of the free axle in $CDCl_3$.

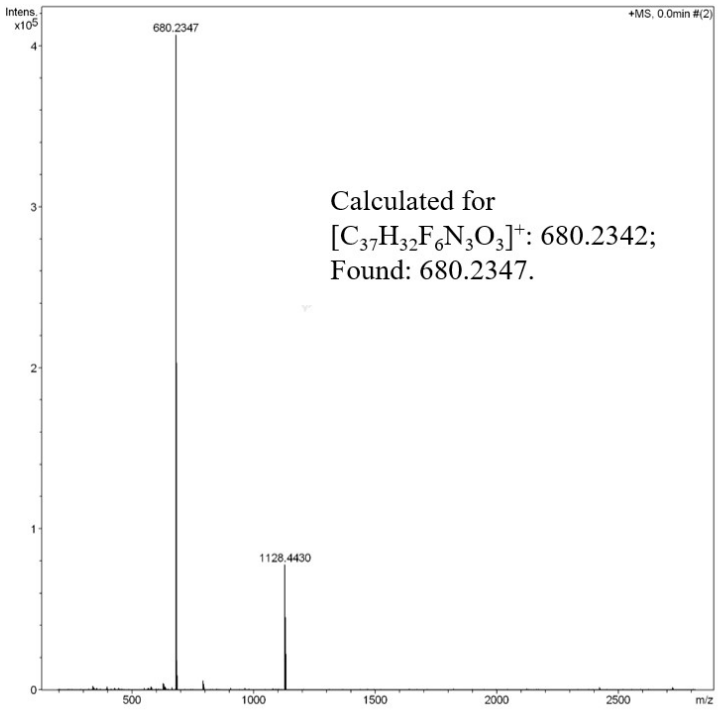

Fig. S21. HRMS spectrum of the free axle.

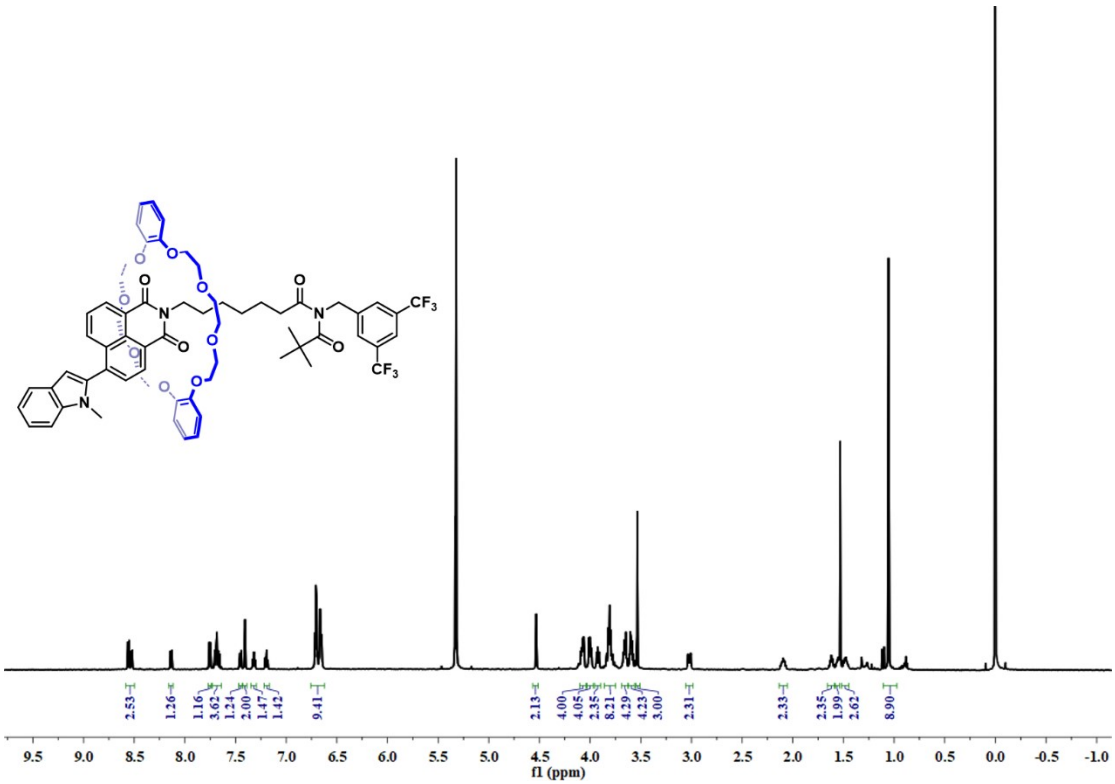

Fig. S22. ^{1}H NMR spectrum of R-1 in CD_2Cl_2.

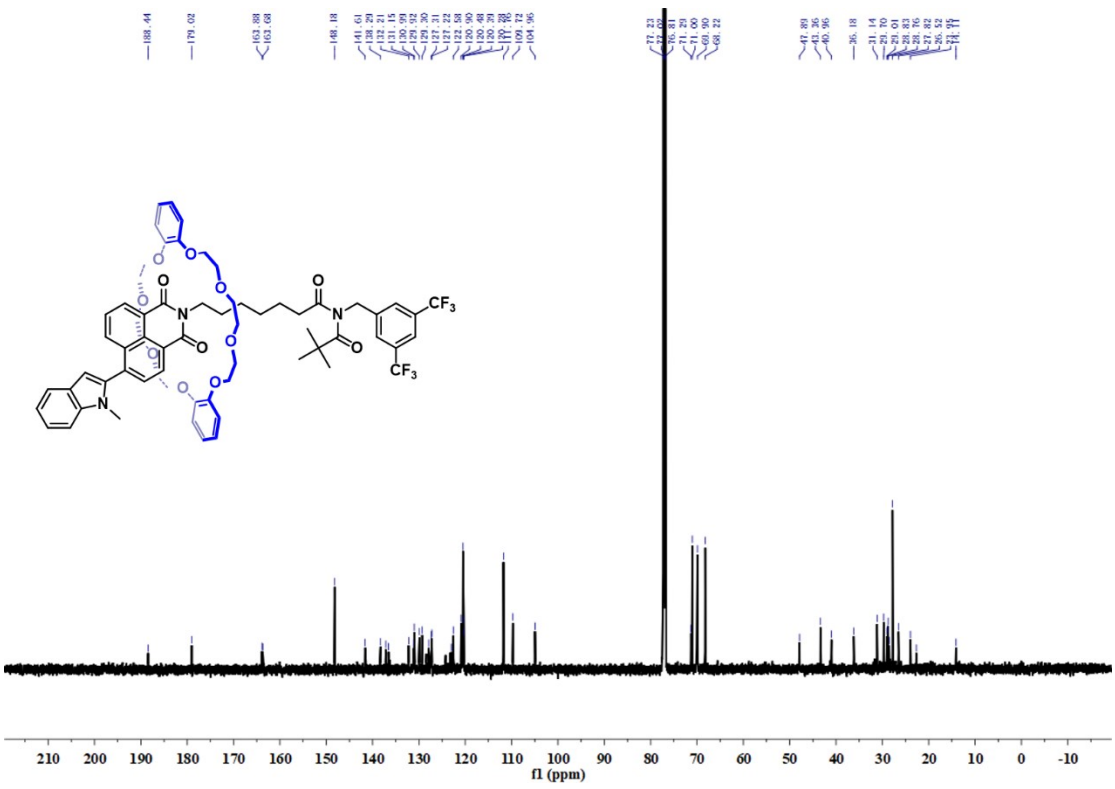

Fig. S23. ^{13}C NMR spectrum of R-1 in $CDCl_3$.

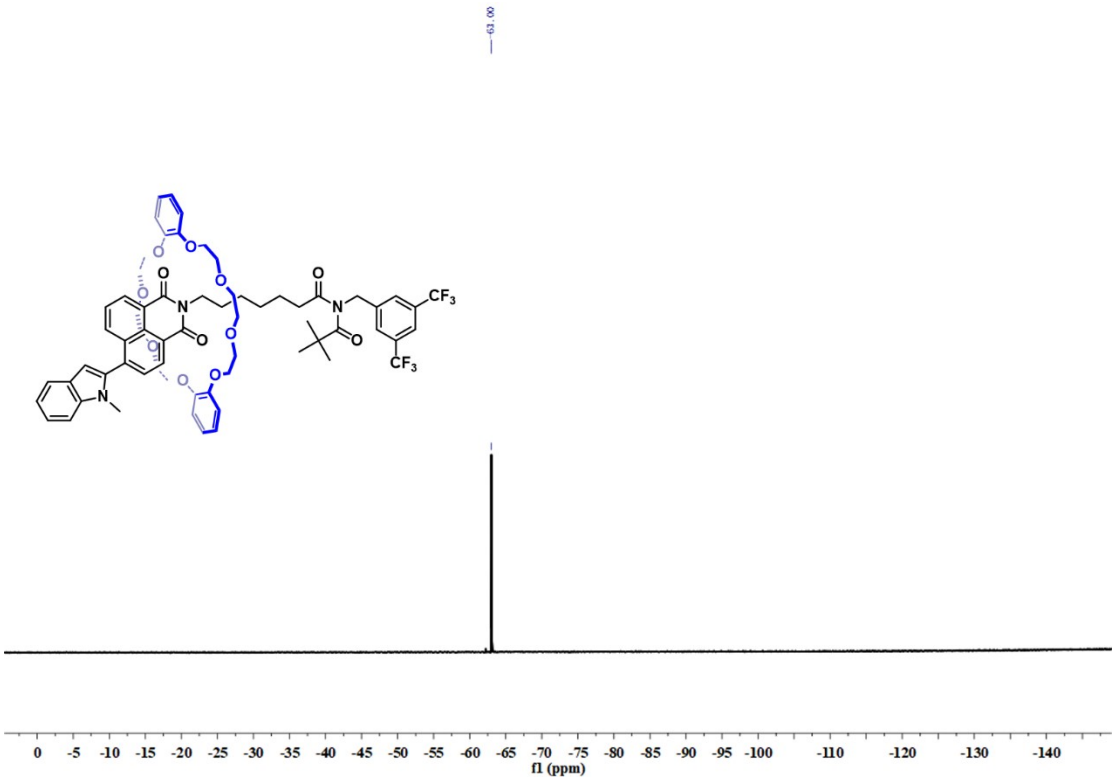

Fig. S24. ^{19}F NMR spectrum of R-1 in CD_2Cl_2.

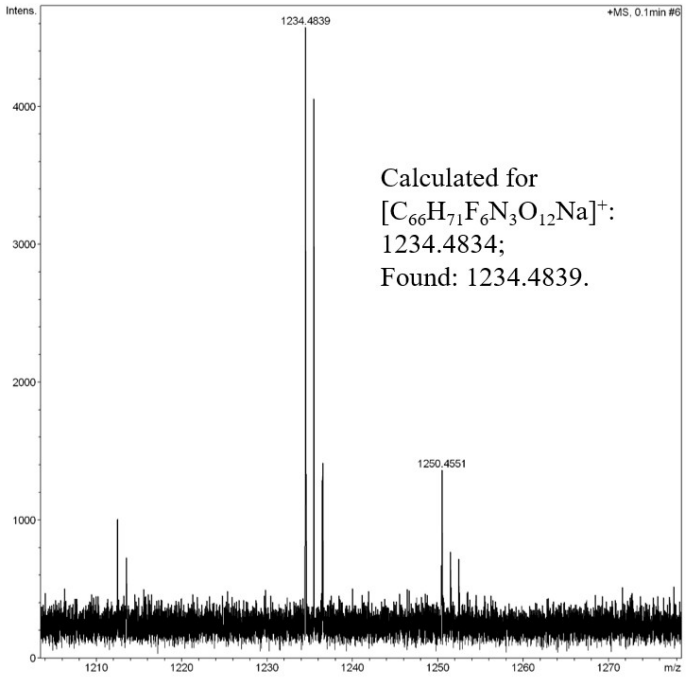

Fig. S25. HRMS spectrum of R-1.

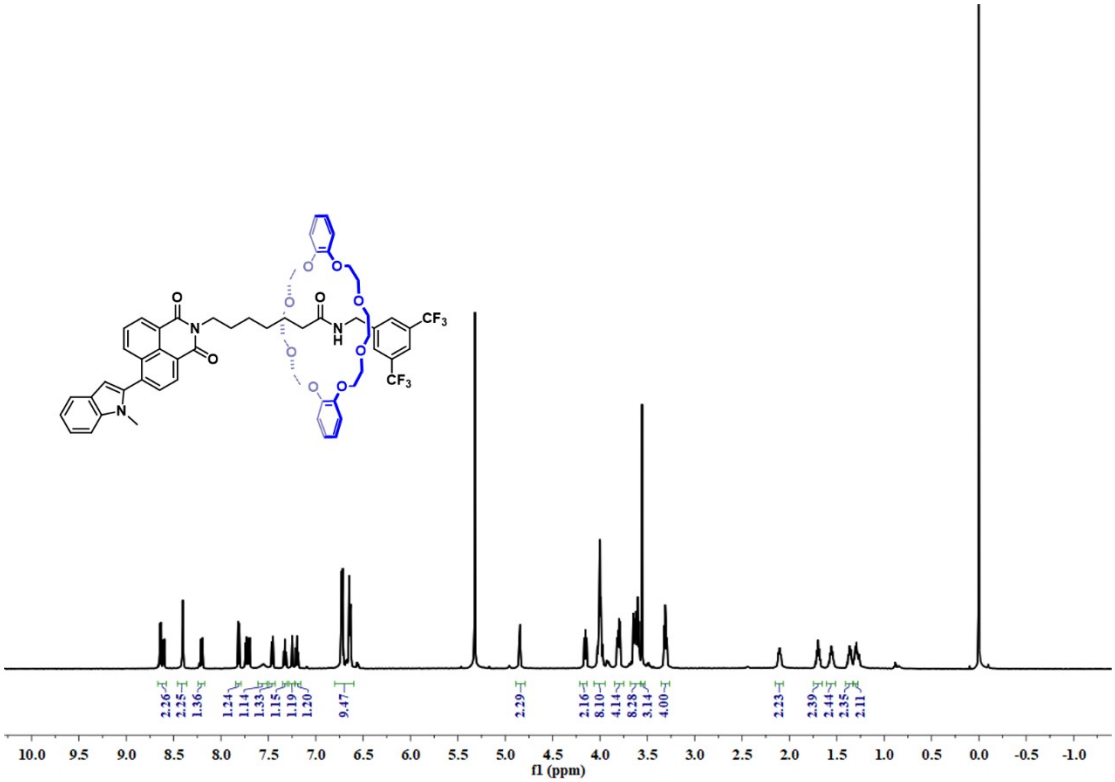

Fig. S26. ^{1}H NMR spectrum of R-2 in CD_2Cl_2.

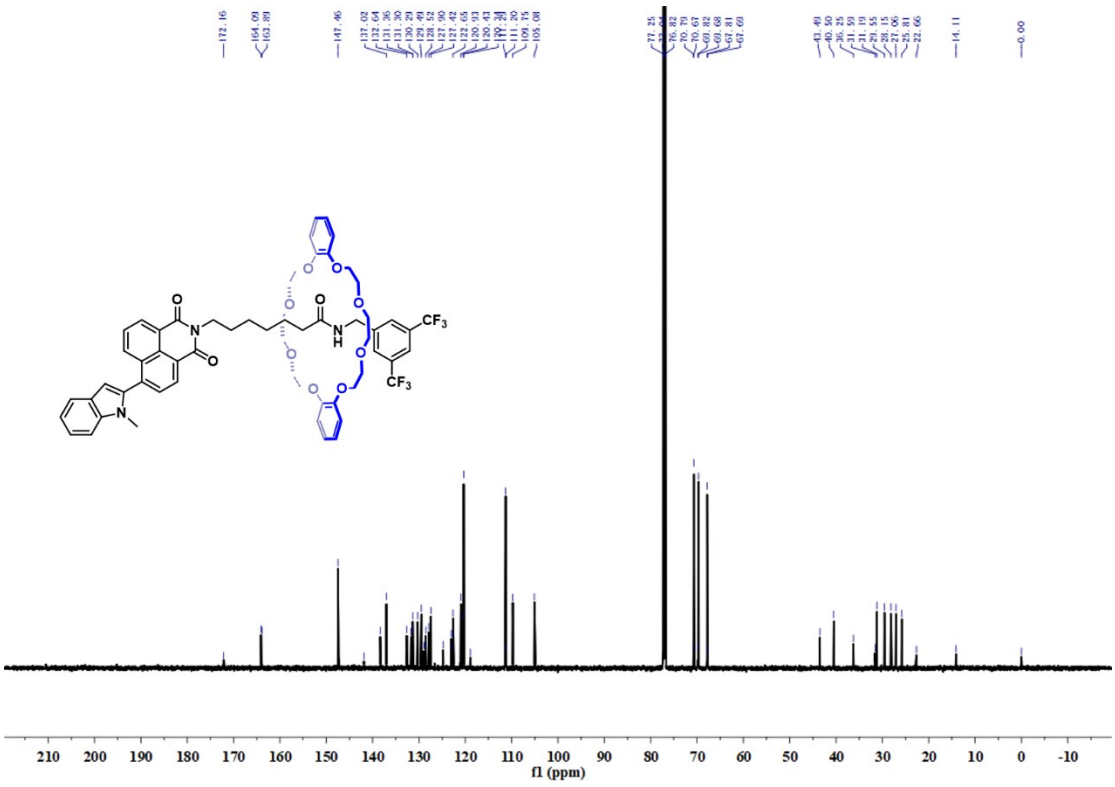

Fig. S27. ^{13}C NMR spectrum of R-2 in $CDCl_3$.

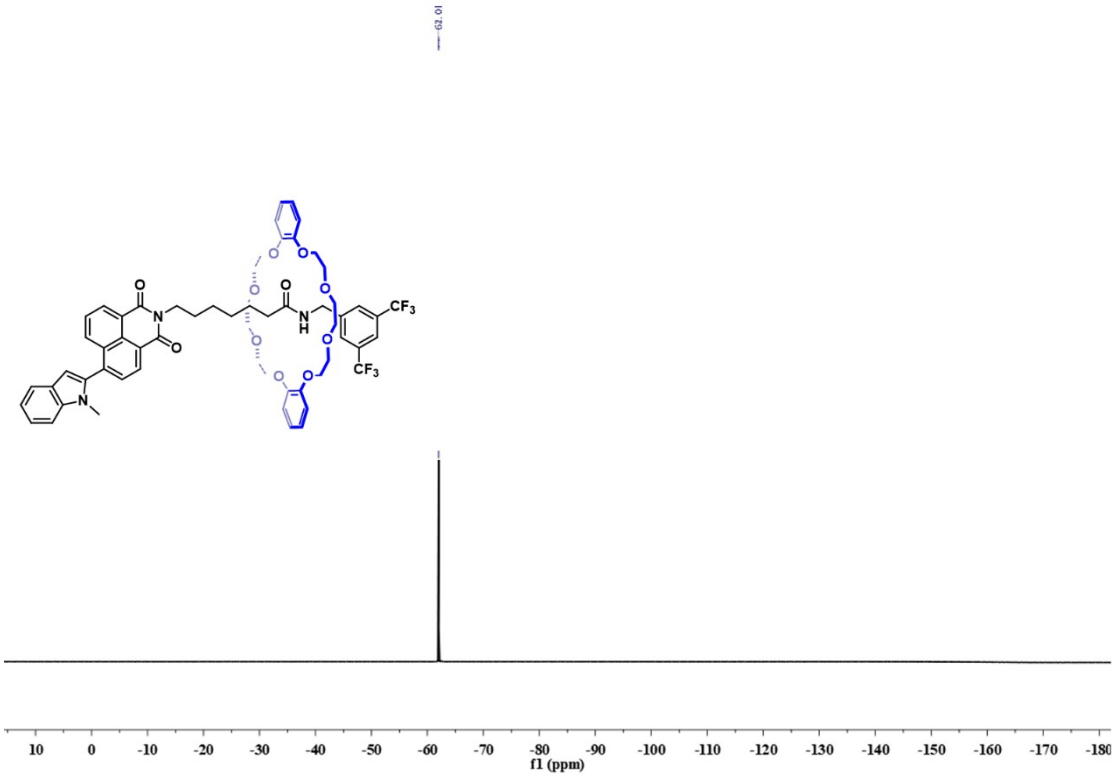

Fig. S28. ^{19}F NMR spectrum of R-2 in $CDCl_3$.

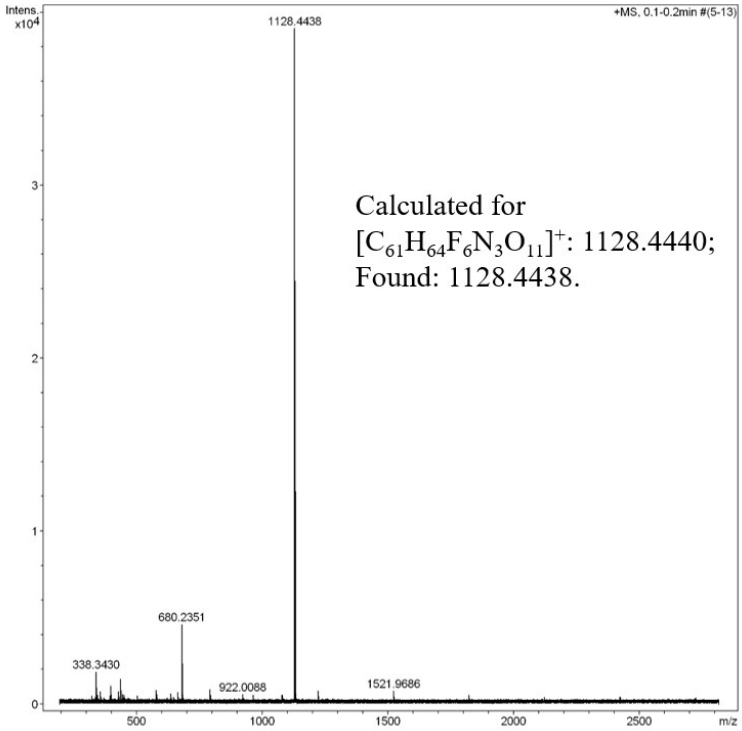

Fig. S29. HRMS spectrum of R-2.

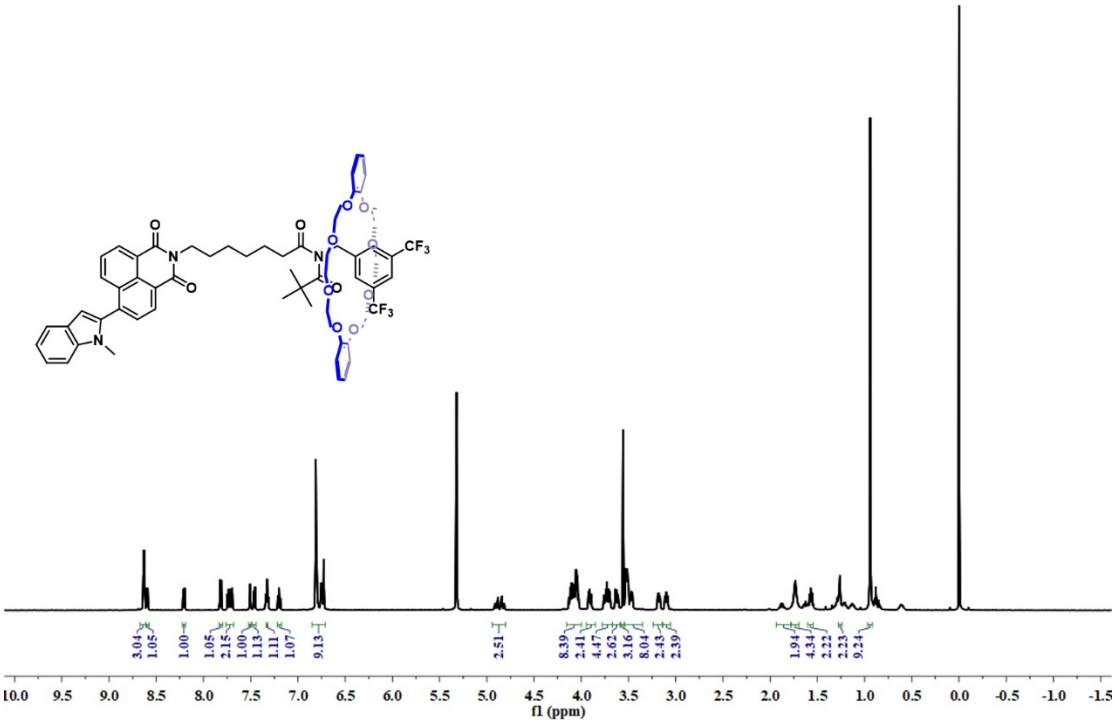

Fig. S30. ^{1}H NMR spectrum of R-3 in CD_2Cl_2.

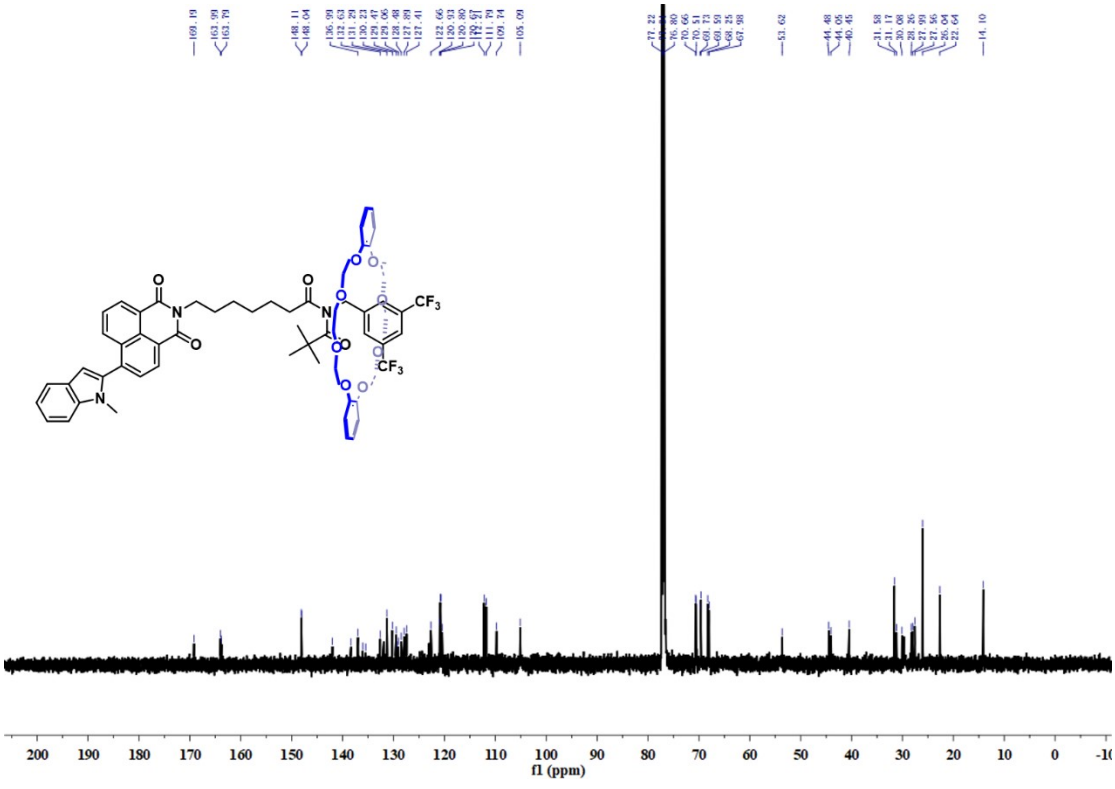

Fig. S31. ^{13}C NMR spectrum of R-3 in $CDCl_3$.

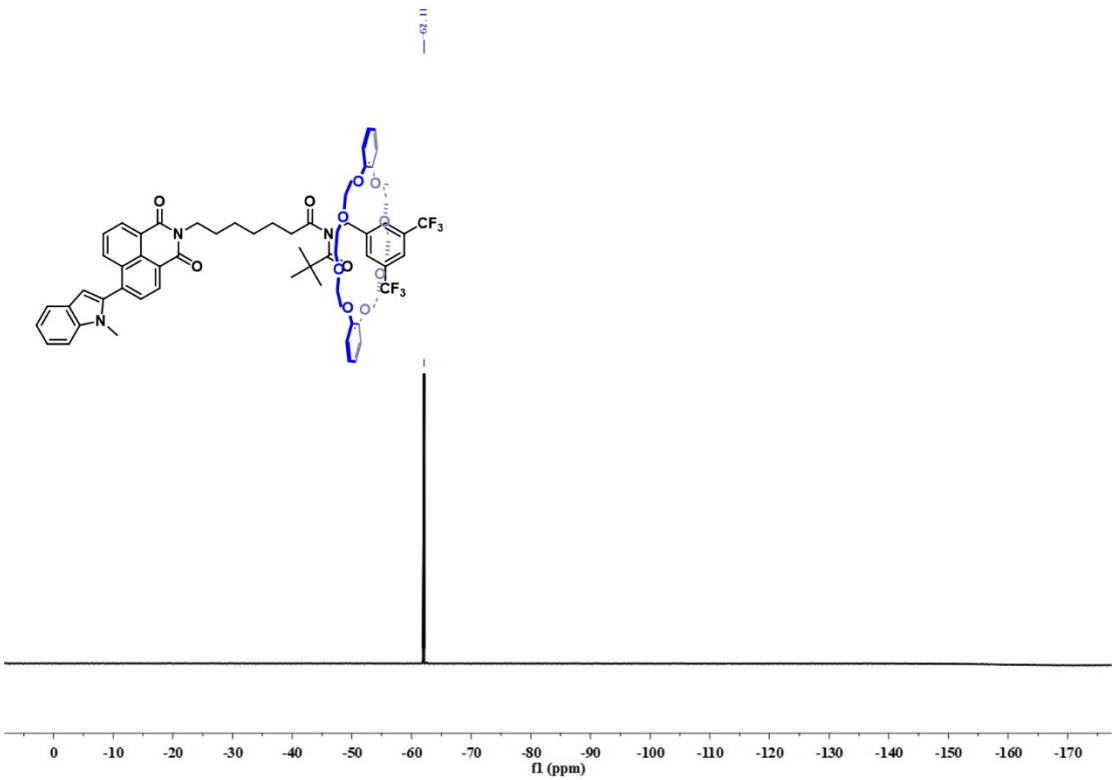

Fig. S32. ^{19}F NMR spectrum of R-3 in $CDCl_3$.

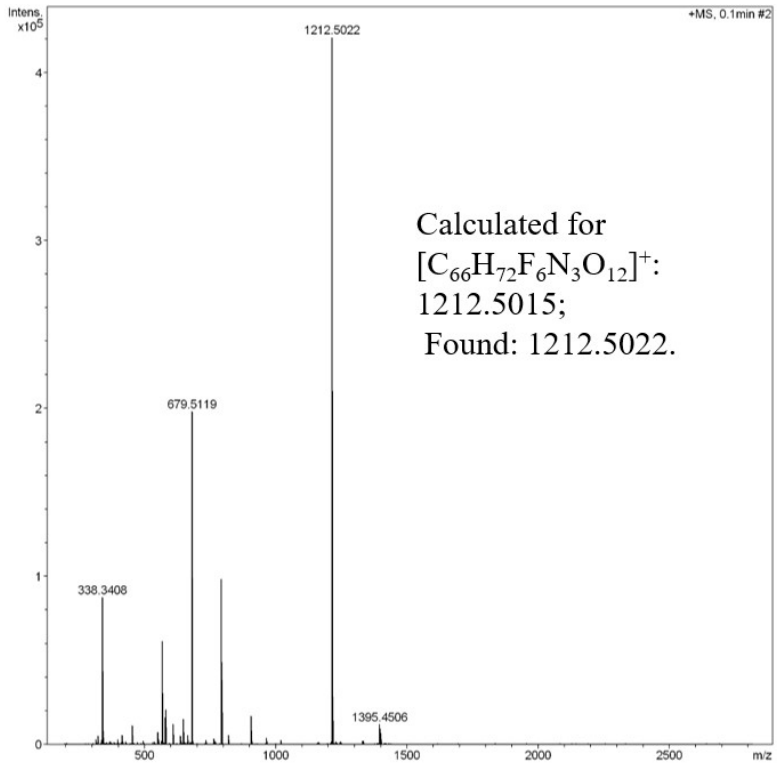

Fig. S33. HRMS spectrum of R-3.

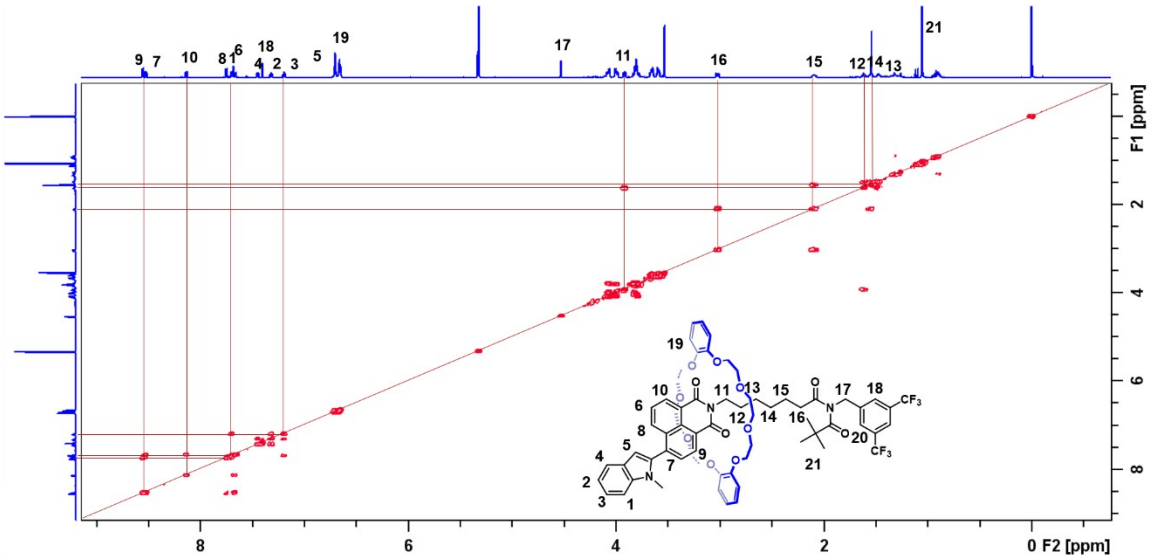

Fig. S34. ^{1}H-^{1}H COSY NMR spectrum of R-1 in CD_2Cl_2.

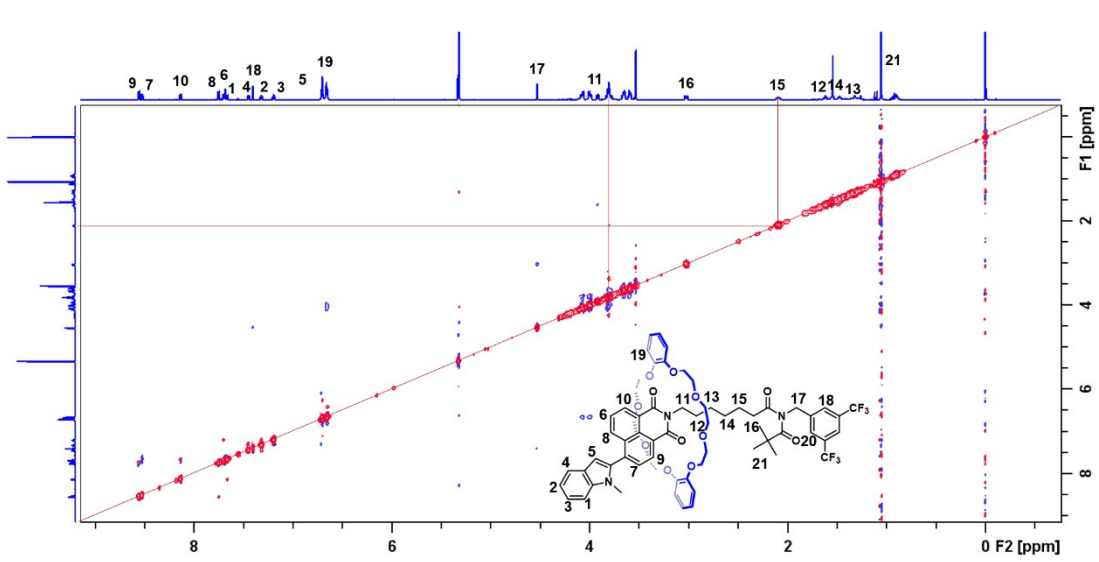

Fig. S35. ^{1}H-^{1}H NOESY NMR spectrum of R-1 in CD_2Cl_2.

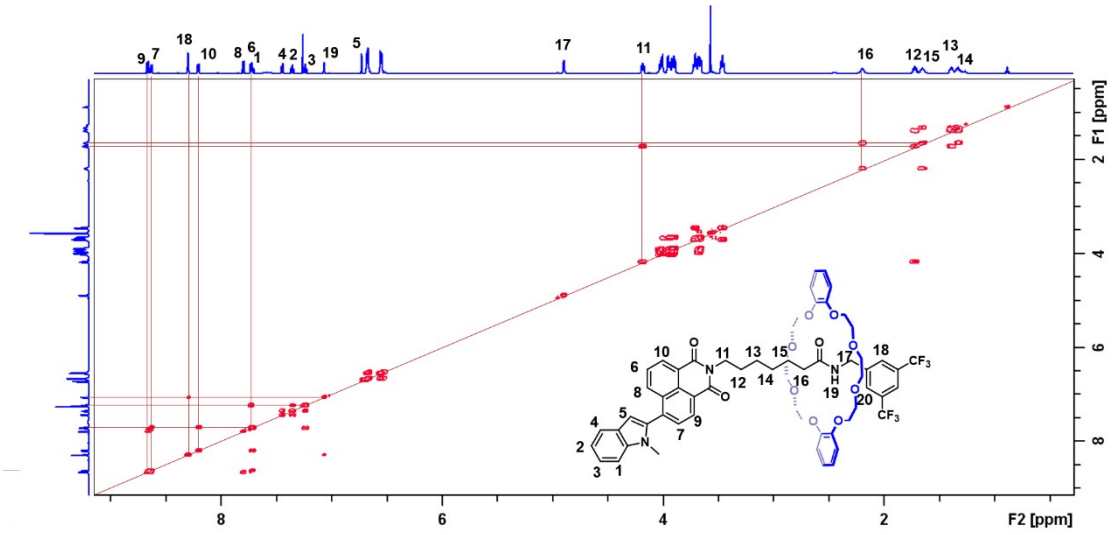

Fig. S36. ^{1}H-^{1}H COSY NMR spectrum of R-2 in $CDCl_3$.

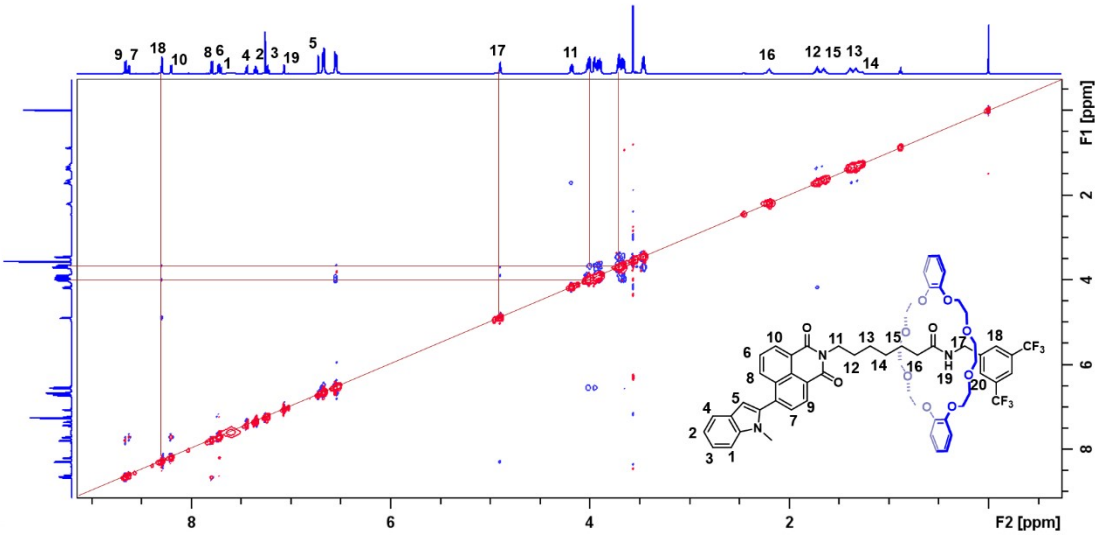

Fig. S37. ^{1}H-^{1}H NOESY NMR spectrum of R-2 in $CDCl_3$.

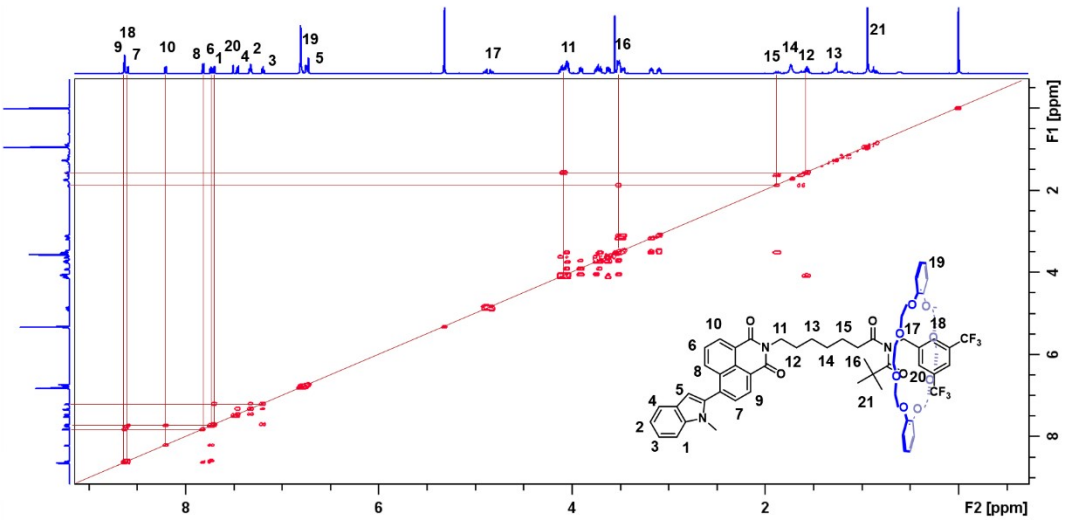

Fig. S38. ^{1}H-^{1}H COSY NMR spectrum of R-3 in CD_2Cl_2.

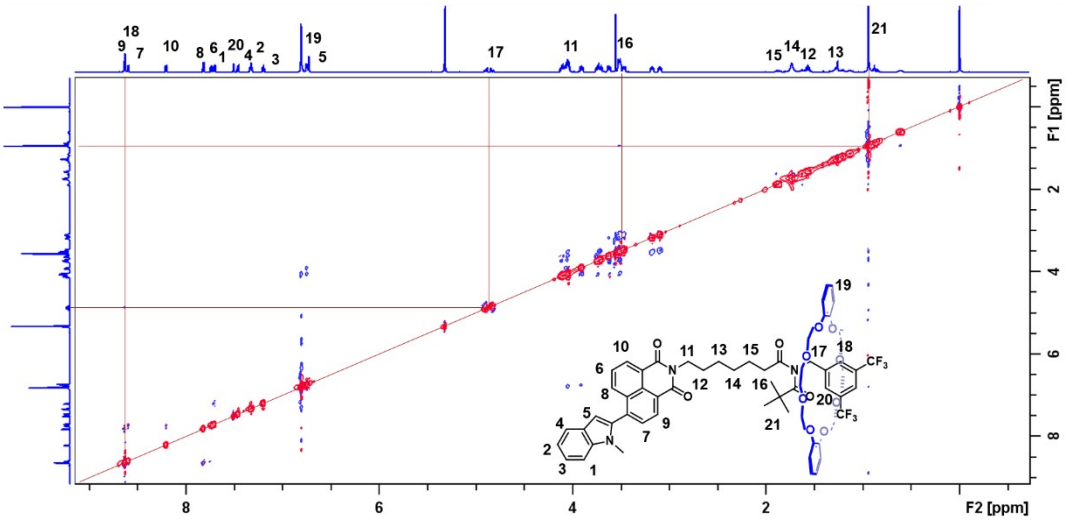

Fig. S39. ^{1}H-^{1}H NOESY NMR spectrum of R-3 in CD_2Cl_2.